

## **Effect of heat input on microstructure and mechanical properties of the TIG welded joints of AISI 304 stainless steel**

T.A.Tabish\*<sup>1</sup> T.Abbas\*, M.Farhan\*, S.Atiq\*, T.Z.Butt\*\*

### **Abstract:**

AISI 304 stainless steel plates were butt-welded through manual tungsten inert gas welding (TIG) process. The process was applied to different specimens by varying heat inputs (low, medium and high). The microstructural features and mechanical properties of the welded joints were examined. The results showed that the tensile strength of welded specimens was greater than that of the base metal. Maximum tensile strength was possessed by the specimen welded using low heat input and vice versa. Microhardness measurements implied that hardness near the upper surface of the weld is high and that near the center of the weld is low because of the faster cooling of the exterior than the interior of the weld. Microhardness increased from 205 VHN to 230 VHN for low heat input, 194 VHN to 211 VHN for medium heat input, and 182 VHN to 195 VHN for high heat input welded specimens. The microstructural study indicated that the high heat input produced larger dendrites than those produced with medium, and low heat input.

### **Keywords:**

Tungsten inert gas are welding, Microstructure, Micro hardness, Tensile Test

### **Introduction:**

Excellent mechanical properties of austenitic stainless steels made them an

important structural material for nuclear plants. Consequently, reactor coolant piping, valve bodies and vessel internals have been manufactured from these steels. However,

welding frequently leads to poor mechanical properties of the weldment due to the metallurgical changes associated with fusion welding processes such as segregation, precipitation of secondary phases, presence of porosities, solidification cracking and grain growth in the heat affected zone (HAZ) etc. [1]. Type 300 series of austenitic stainless steels contain considerable amounts of chromium and nickel; the former provides corrosion resistance and the latter stability of austenite phase at room temperature. The basic composition of traditional austenitic stainless steel includes 18% chromium and 8% nickel, but can also include small proportions of molybdenum, titanium, niobium, copper and nitrogen. Other useful properties of engineering significance such as excellent corrosion resistance, superior creep rupture strength and impact resistance at low temperatures make austenitic stainless steels a competitive choice for industrial plants encompassing applications in chemical processing, food production, marine hardware, furnaces, heat exchangers, gas turbines, and cryogenic vessels.

To fabricate stainless steel structures, welding is generally the most convenient process. But the common arc welding results in coarse grains and carbides formation along the grain boundaries in HAZ. Both the

coarser structure and carbides, which are rich in chromium, deteriorate the mechanical properties of the weldment [2,3]. Therefore, type 300 series is often joined through gas tungsten arc welding (GTAW), also known as tungsten inert gas (TIG) welding, essentially consisting of production of an arc between a non-consumable tungsten electrode and the work piece. An inert gas, usually argon, protects the arc, electrode and molten pool from atmospheric contamination. While joining the thinner surfaces, edge joints and flanges, filler metals are generally not required. However, for thicker cross-sections, a filler metal is needed to feed the joint. TIG welding is equally capable of joining thin as well as thick materials to achieve quality welds for materials ranging from stainless steels to non-ferrous alloys. TIG welding has some limitations as compared to gas metal arc welding (GMAW), major being inferior joint penetration and poor tolerance to many material compositions [4,5]. However, penetrating ability of activated TIG arc can markedly be improved by applying fluxes, generally composed of oxides of Mn, Mo, Ti, Si and Al, on surfaces prior to welding [6 – 8]. However, the primary drawback of TIG welding process is its inability to join thicker surfaces in a single pass. For butt-

joint penetration, multi-pass technique must be used when thickness of stainless steel plates to be joined exceeds 3mm [2,8]. The laser-TIG hybrid welding overcomes these limitations allowing improved welding stability and greater melting efficiency [1].

In preceding studies, joints made from the TIG welding process have not been examined in detail with reference to microhardness varying across the joint. The present work expatiates the TIG joints of AISI 304 stainless steel plates through

microstructural observations and mechanical properties.

**Materials and Experimental Procedures:**

AISI 304 stainless steel plates of sizes 200mm x 100mm x 6mm cut from a rolled sheet and the filler 308 stainless steel solid electrode EW-Th-2 (thoriated tungsten) of 3.15 mm diameter were utilized for this study. The measured compositions of base and filler materials are given in Table 1.

**Table 1. Composition of Base & Filler Material**

| Alloy  | C    | Si   | Mn   | P     | S     | Cr    | Ni    | Fe      |
|--------|------|------|------|-------|-------|-------|-------|---------|
| 304 SS | 0.07 | 0.41 | 1.89 | 0.03  | 0.015 | 18.6  | 8.48  | Balance |
| 308 SS | 0.08 | 1.0  | 1.59 | 0.045 | 0.03  | 18.10 | 10.09 | Balance |

Argon gas was used as shielding medium during the TIG Welding and the pressure was maintained at 15 L/min. Cleaning of the surfaces to be joined was accomplished by a combination of vapor and liquid cleaners. Samples were supported by conventional fixtures to facilitate smooth welding. The conditions used during the TIG welding process are mentioned in

**Table 2 (a – c)** for samples welded at low, medium and high heat respectively.

**Table 2 (a) Process Parameters used for fabrication butt welded joints (Low Heat)**

| Side of Plate | Pass         | Current (A) | Voltage (V) | Average Welding Speed (mm/min) | Average Heat input per unit length per pass (kJ/mm) | Total heat input per unit length of the weld (kJ/mm) |
|---------------|--------------|-------------|-------------|--------------------------------|---|--|
| Side A        | Root Pass    | 125         | 30          | 2.2                            | 1.02  | 4.96   |
|               | Hot Pass     | 125         | 30          | 2.3                            | 0.98  |  |
|               | Capping Pass | 125         | 30          | 2.6                            | 0.87  |  |
| Side B        | Filling Pass | 125         | 30          | 2.2                            | 1.02  |  |
|               | Capping Pass | 125         | 30          | 2.1                            | 1.07  |  |

Table 2 (b) Process Parameters used for fabrication butt welded joints (Medium Heat)

| Side of Plate | Pass         | Current (A) | Voltage (V) | Average Welding Speed (mm/min) | Average Heat input per unit length per pass (kJ/mm) | Total heat input per unit length of the weld (kJ/mm) |
|---------------|--------------|-------------|-------------|--------------------------------|---|--|
| Side A        | Root Pass    | 155         | 35          | 3.01                           | 1.08  | 5.41   |
|               | Hot Pass     | 155         | 35          | 3.005                          | 1.08  |  |
|               | Capping Pass | 155         | 35          | 3.03                           | 1.07  |  |
| Side B        | Filling Pass | 155         | 35          | 2.999                          | 1.09  |  |
|               | Capping Pass | 155         | 35          | 3.01                           | 1.08  |  |

Table 2 (c) Process Parameters used for fabrication butt welded joints (High Heat)

| Side of Plate | Pass         | Current (A) | Voltage (V) | Average Welding Speed (mm/min) | Average Heat input per unit length per pass (kJ/mm) | Total heat input per unit length of the weld (kJ/mm) |
|---------------|--------------|-------------|-------------|--------------------------------|---|--|
| Side A        | Root Pass    | 185         | 40          | 3.88                           | 1.14  | 5.82   |
|               | Hot Pass     | 185         | 40          | 3.784                          | 1.17  |  |
|               | Capping Pass | 185         | 40          | 3.7                            | 1.20  |  |
| Side B        | Filling Pass | 185         | 40          | 3.901                          | 1.14  |  |
|               | Capping Pass | 185         | 40          | 3.81                           | 1.17  |  |

The specimens used for tensile testing, microstructure study, and micro-hardness testing were sectioned, cleaned, grounded, polished and electrolytically etched. An electrolytic oxalic acid (10g) with distilled water (100mL) supplied with a cell voltage of 6 V with etching time of 1 min was provided for electrolytic etching of the sample. The microstructure was finally examined by optical microscope (METKON IMM901). The specimens were tested on a computerized tensile testing machine of 100KN capacity with very slow strain rates

( $\epsilon=10^{-4}$  to  $10^{-2}$  s<sup>-1</sup>). Hardness distribution at transverse and longitudinal axis on the joints was measured using a Vickers hardness tester (FM-800) with testing load and holding time of 1 kg and 15 s respectively.

**Results & Discussions:**

The ultimate tensile strength (UTM) values, % elongation and weld efficiencies are mentioned in **Table 3**.

**Table 3 Tensile Test Result**

| Sample No. | Tensile Properties              |                           | Location of Fracture | Joint Efficiency (%) |
|------------|---------------------------------|---------------------------|----------------------|----------------------|
|            | Ultimate Tensile Strength (MPa) | Percentage Elongation (%) |                      |                      |
| Base Metal | 609.68                          | 40                        | -                    | -                    |
| 1          | 655                             | 25                        | Base Metal           | 107.4                |
| 2          | 643.02                          | 23                        | Base Metal           | 105.5                |
| 3          | 620.4                           | 22                        | Base Metal           | 101.8                |

Sample 1: Welded at Low Heat Input, Sample 2: Welded at Medium Heat Input, Sample 3: Welded at High Heat Input.

Results showed that, in each case, the tensile strength of welded specimen is greater than that of the base metal. Maximum tensile strength is possessed by the specimen which was welded using low heat input and the converse was observed in case of high heat input. All the three welded samples fractured at the base metal which is the indication of the higher tensile strength of the weld. A similar study [9], employing

current of 80 A (much lower than that applied in this work), found tensile strength of the weldment about 1800 MPa. Hence it can be inferred that tensile strength inversely relates to electrode current provided that welding speed remains comparable. Weld efficiency of the specimen employed low heat input was greater than other ones. Microhardness measurement results, graphically represented in **Figure 1 (a and b)**, illustrated that the hardness varied as the

probe traversed from the surface of the weld to its center.

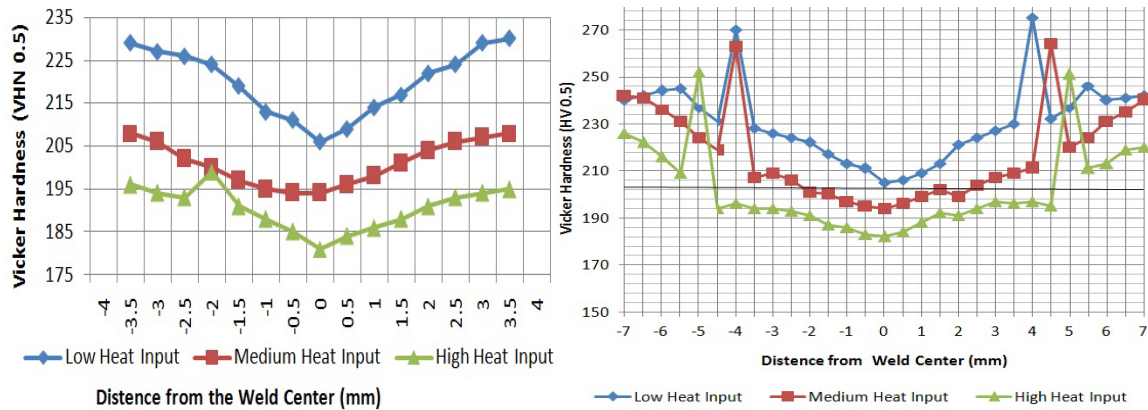


Figure 1 Microhardness a and b in Transverse Direction and longitudinal directions respectively

Comparatively faster cooling rate hardened the upper surface of the weld. As the indenter moved away from the center of the weld towards the fusion zone, microhardness increased from 205 VHN to 230 VHN for low heat input, 194 VHN to 211 VHN for medium heat input and 182 VHN to 195 VHN for high heat input welded specimen. Proportionate hardness values were reported in another work [9]. The phenomenon of decrease in hardness of the weldment with increasing heat input is specific for TIG welding [10]. While moving away from the weld towards the fusion zone, fusion boundary came across which was responsible for the abrupt increase in hardness values of 275 VHN, 264 VHN and 251 VHN for low, medium

and high heat input respectively. High hardness of the fusion boundary was because of the presence of the partially melted grains. After reaching the maximum hardness value, the hardness decreased in the heat affected zone (HAZ). In all the welds, area adjacent to the fusion boundary (heat affected zone) was coarse grained which possessed low hardness whereas the heat affected zone adjacent to the base metal was fine grained which possessed high hardness. The reason for this trend of microhardness is the heat affected zone experienced slow cooling rate and hence had coarse grained microstructure, whereas the area adjacent to base metal went through faster cooling rate and hence fine grained microstructure was obtained. Microhardness values of specimens using low, medium and

high heat input are given in **Table 4 (a and b)** respectively.

**Table 4 a Microhardness Values in Transverse Direction for low, medium, & High Heat input**

| Distance from Weld Center | Micro-Hardness (HV 0.5)  |                              |                            |
|---------------------------|--------------------------|------------------------------|----------------------------|
|                           | Sample 1(Low Heat Input) | Sample 2 (Medium Heat Input) | Sample 3 (High Heat Input) |
| -3.5                      | 229                      | 208                          | 196                        |
| -3                        | 227                      | 206                          | 194                        |
| -2.5                      | 226                      | 202                          | 193                        |
| -2                        | 224                      | 200                          | 199                        |
| -1.5                      | 219                      | 197                          | 191                        |
| -1                        | 213                      | 195                          | 188                        |
| -0.5                      | 211                      | 194                          | 185                        |
| 0                         | 206                      | 194                          | 181                        |
| 0.5                       | 209                      | 196                          | 184                        |
| 1                         | 214                      | 198                          | 186                        |
| 1.5                       | 217                      | 201                          | 188                        |
| 2                         | 222                      | 204                          | 191                        |
| 2.5                       | 224                      | 206                          | 193                        |
| 3                         | 229                      | 207                          | 194                        |
| 3.5                       | 230                      | 208                          | 195                        |
| 4                         |                          |                              |                            |

**Table 4 b Microhardness values in Longitudinal Direction for low, medium, and high heat input**

| Distance from Weld Center | VICKER HARDNESS (HV0.5)   |                              |                            |
|---------------------------|---------------------------|------------------------------|----------------------------|
|                           | Sample 1 (low heat input) | Sample 2 (medium heat input) | Sample 3 (high heat input) |
| -7                        | 240                       | 242                          | 226                        |
| -6                        | 244                       | 236                          | 216                        |
| -5                        | 237                       | 224                          | 252                        |
| -4                        | 270                       | 263                          | 196                        |
| -3                        | 226                       | 209                          | 194                        |
| -2                        | 222                       | 201                          | 191                        |
| -1                        | 213                       | 197                          | 186                        |
| 0                         | 205                       | 194                          | 182                        |
| 1                         | 209                       | 199                          | 188                        |
| 2                         | 221                       | 199                          | 191                        |
| 3                         | 227                       | 207                          | 197                        |

|   |     |     |     |
|---|-----|-----|-----|
| 4 | 275 | 211 | 197 |
| 5 | 237 | 220 | 251 |
| 6 | 240 | 231 | 213 |
| 7 | 242 | 240 | 220 |

Full penetration welds were obtained in all samples made using low, medium, and high heat input. It became evident from the microstructures that the area of heat affected zone (HAZ) was proportional to the heat input. An addition to heat input increased

the area of heat affected zone correspondingly. Optical micrographs, given in **Figure 2 (a – c)**, revealed the microstructures of weld zone, fusion boundary and heat affected zone (HAZ) for different heat input combinations.



**Fig 2 Microstructure a,b and c showing HAZ, Fusion Boundary, & Weld Metal Low Heat Input, medium heat and high heat input respectively**

It is clear from the microstructures that the high heat input produced larger dendrites. In case of low heat input, the cooling rate was faster so there was lesser time for the dendrites to grow resulting in finer microstructure. Similar reason was responsible for smaller dendritic structure when laser-TIG process was practiced [1].

**Conclusion:**

Butt-joints of AISI 304 stainless steel plates were developed by exercising manual TIG welding process and

consequently detailed out in order to evaluate their microstructure and mechanical properties for different conditions of low, medium and high inputs. The major results exhibited that the weldment was stronger than the base metal and strength varies across the joint, maximum being at the surface of the same. The process using low heat input produced fine structured fusion and heat affected zones which in turn performed vigorously under applied stress thereby offering greater strength and hardness.



T.A.Tabish, Institute of Advanced Materials,  
Bahauddin Zakariya University, 60800,  
Multan.Pakistan

T.Abbas, Institute of Advanced Materials,  
Bahauddin Zakariya University, 60800,  
Multan.Pakistan

M.Farhan, Institute of Advanced Materials,  
Bahauddin Zakariya University, 60800,  
Multan.Pakistan

S.Atiq, Institute of Advanced Materials,  
Bahauddin Zakariya University, 60800,  
Multan.Pakistan

T.Z.Butt, Faculty of Engineering and  
Technology, University of the Punjab, 54590,  
Lahore, Pakistan

<sup>1</sup> Corresponding author: email  
address: [engrtanvir@bzu.edu.pk](mailto:engrtanvir@bzu.edu.pk) (T.A.Tabish)

## References:

[1] Jun Yan, Ming Gao, Xiaoyan Zeng,  
Study on microstructure and mechanical  
properties of 304 stainless steel joints by  
TIG, laser and laser-TIG hybrid welding  
Optics and Lasers in Engineering, 48 (2010)  
512–517

[2] T. Sakthivel, M. Vasudevan, K. Laha, P.  
Parameswaran, K.S. Chandravathi, M.D.  
Mathew, A.K. Bhaduri, Comparison of  
creep rupture behaviour of type 316L(N)  
austenitic stainless steel joints welded by  
TIG and activated TIG welding processes  
Materials Science and Engineering A, 528  
(2011) 6971– 6980

[3] P. Sathiya, S. Aravindan, A. Noorul Haq,  
Effect of friction welding parameters on

mechanical and metallurgical properties of  
ferritic stainless steel, The International  
Journal of Advanced Manufacturing  
Technology, 31, 11-12 (2007) 1076–1082

[4] Hidetoshi Fujii, Toyoyuki Sato,  
Shanping Lua, Kiyoshi Nogi, Development  
of an advanced A-TIG (AA-TIG) welding  
method by control of Marangoni convection,  
Materials Science and Engineering A, 495  
(2008) 296–303

[5] Zhiguo Gao, Yixiong Wu, Jian Huang,  
Analysis of weld pool dynamic during  
stationary laser–MIG hybrid welding, The  
International Journal of Advanced  
Manufacturing Technology, 44, 9-10,(2009)  
870-879

[6] Paskell, T., Lundin, C. & Castner, H.  
Gtaw flux increases weld joint  
penetration. Welding Journal, 76 (1997) 4,  
57–62,

[7] M. Tanaka, T. Shimizu, T. Terasaki, M.  
Ushio, F. Koshiishi, C.-L Yang, Effects of  
activating flux on arc phenomena in gas  
tungsten arc welding, Science and  
Technology of Welding & Joining, 5 (2000)  
6, 397-402

[8] Kuang-Hung Tseng, Chih-Yu Hsu,  
Performance of activated TIG process in

austenitic stainless steel welds Journal of  
Materials Processing Technology, 211  
(2011) 503–512

[9] Halil İbrahim Kurt<sup>1</sup>, Ramazan Samur,  
Study on Microstructure, Tensile Test and  
Hardness 304 Stainless Steel Jointed by TIG  
Welding, International Journal of Science  
and Technology, 2 (2013) 163-168

[10] L.S. Kumar<sup>1</sup>, S.M.Verma, P.R.K.  
Prasad, P.K. Kumar, T.S. Shanker,  
Experimental Investigation for Welding  
Aspects of AISI 304 & 316 by Taguchi  
Technique for the Process of TIG & MIG  
Welding, International Journal of  
Engineering Trends and Technology, 2  
(2011) 28-33

IJSER